agronomy

MDPI

Article

CFD Simulation and Experiments of Pneumatic Centralized Cylinder Metering Device Cavity and Airflow Distributor

Baolong Wang [1], Yi Na [1], Yihong Pan [1], Zhenbo Ge [1], Jian Liu [1] and Xiwen Luo [2,*]

[1] School of Horticulture, Hainan University, Haikou 570228, China; wangbaolong@hainanu.edu.cn (B.W.); nygreeny@163.com (Y.N.); pyh159263@163.com (Y.P.); 15595672663@163.com (Z.G.); liujian99@hainanu.edu.cn (J.L.)

[2] Key Laboratory of Key Technology on Agricultural Machine and Equipment, Ministry of Education, South China Agricultural University, Guangzhou 510642, China

* Correspondence: xwluo@scau.edu.cn

Abstract: The distribution of airflow field in the pneumatic centralized cylinder metering device cavity, airstream distributor and different angle seed feeding tubes was investigated based on the pneumatic centralized cylinder direct-seeding metering device to study the effect on the movement law of rice seed. In total, three suction hole sizes (1.5 mm, 2 mm and 2.0 mm 45° wedge) were used for CFD simulation. The results showed that under the same inlet vacuum, the pressure at the 1.5 mm hole is higher than the other two types of holes, and the five measurement points of the 2 mm hole are more stable than the other two types of holes. At the positive pressure seed feeding area, the inlet pressure was set as 1.5 kPa, and the outlet pressure was set as 0 Pa. The pressure distribution at different measuring points showed that the 2 mm 45° wedge had the most uneven positive pressure distribution, and the 1.5 mm hole had higher positive pressure distribution than the 2 mm hole in general. Three different structured airflow distributors were designed. CFD simulation experiments showed that the arc transition type presented better uniformity than the other two types. The uniformity experiments at the ends of the seed-feeding tubes indicated that the airflow velocity had the trend of large in the middle and small at two sides. Finally, the movement law of the rice seeds in seed feeding tubes at different angles was obtained by using high-speed photography. The results showed that the rice seeds in tube C (maximum angle) presented a movement posture of falling sector a and kept falling after colliding in sector b; the rice seeds in tube B (the second angle) presented a movement posture of falling in sector a and kept falling after colliding in sector b. The above research provides a reference for the optimal design of a pneumatic centralized cylinder metering device.

Keywords: CFD simulation; experiments; centralized cylinder metering device; cavity; airflow distributor

check for updates

Citation: Wang, B.; Na, Y.; Pan, Y.; Ge, Z.; Liu, J.; Luo, X. CFD Simulation and Experiments of Pneumatic Centralized Cylinder Metering Device Cavity and Airflow Distributor. *Agronomy* **2022**, *12*, 1775. https://doi.org/10.3390/agronomy12081775

Academic Editors: Hua Li, Lizhang Xu and Andrea Peruzzi

Received: 8 June 2022
Accepted: 26 July 2022
Published: 28 July 2022

Publisher's Note: MDPI stays neutral with regard to jurisdictional claims in published maps and institutional affiliations.

Copyright: © 2022 by the authors. Licensee MDPI, Basel, Switzerland. This article is an open access article distributed under the terms and conditions of the Creative Commons Attribution (CC BY) license (https://creativecommons.org/licenses/by/4.0/).

1. Introduction

With the popularization of rice direct seeding more and more widely, the mechanized direct-seeding technology has achieved significant development in recent years, of which the precision rice hill–drop drilling technology has been promoted over a wide area due to its advantages of saving time and work, well-ventilated fields, fewer pests, low tillering node in rice and even growth [1–4]. Hybrid rice, owing to its features of strong tillering ability and high production, is one of the most popular varieties. The planting area of hybrid rice has reached 16.1787 million hectares, accounting for 53.37% of the total planting area of rice in China [5,6]. Current mechanical seed-metering device is mainly designed for medium or large seeding amounts requirements, which is hard to meet the requirements of precise seeding of hybrid rice.

A pneumatic seed-metering device is suitable for precise seeding due to its characteristics of less bud damage and strong adaptability to the dimensions of rice seeds. In order to

improve the performance of seed-metering devices, intensive studies have been conducted recently to investigate the distribution and suction mechanism of material particles in the seed suction process of the seed-metering device. A vertical disc seed-metering device with the linear-type and guide-type seed-stirring mechanism was experimented. High speed photography technology is used to record the posture of rice seeds [7–10]. A pneumatic centralized seed-stirring device for rapeseed and wheat was developed, the major factors of the seed-stirring device affecting the seed filling performance were analyzed, the main structural parameters of the stirring device and stirring axle were determined, and the impact of the structure and configuration of the stirring device on the filling performance was investigated by means of DEM simulated analysis and a bench experiment, which provides a reference to the hill-drop pneumatic central cylinder direct-seeding machine [11]. The discrete element method was applied to perform simulated analysis on the seed distribution in the seed-metering device, acting force between seeds, and moving speed of seeds. Theoretical analysis is used to calculate the posture of rice seeds [12]. Extensive studies have been conducted on the working parameters of cylinder seed-metering device during the seed-suction process, but the studies on the pneumatic cylinder seed-metering device did not involve hybrid rice nor did they include the design criteria of the seed-metering device, CFD simulation method and parameter selection, etc. [13–19].

To meet the requirement of the precision direct seeding for hybrid rice, a hill-drop pneumatic central cylinder direct-seeding machine to sow ten rows at a time was designed. A series of field experiments were then conducted to test the seeder performance according to national standard test methods, and the field test results showed that for the hill-drop pneumatic central cylinder direct-seeding machine, the probability of (2 $\pm$ 1) seeds in each hill was 91.6%, while the probability of the missing hill was 2.7% [20–22]. A reasonable combination of distributed conveyor type seed feeding tubes and airflow parameters is critical to determine the seed-metering uniformity of the pneumatic centralized cylinder direct-seeding machine. This paper performed a CFD simulation analysis and experimental study on the pneumatic centralized cylinder metering device cavity, the airstream distributor and the seed-feeding tubes. The pressure distribution and velocity distribution (such as streamline distribution of velocity flow field) of the metering device cavity were used as referring indicators, and the different angle seed-feeding tubes and air velocity parameters were used as influence factors for the study of the colliding law of rice seeds in seed feeding tubes.

2. Material and Methodology

2.1. Structure and Working Principle

According to the technical requirements of rice hill-drop direct seeding (per-hill 2 $\pm$ 1 rice seeds), a vacuum central drum seed metering device is designed [20,21], which is mainly composed of seed box 1, outer cylinder 2 (replaceable outer cylinder for different parameter of sucking holes), ventilation shell 3 (connecting the positive and negative with fan respectively), seeding tubes 4 (seed discharged channel), and airflow delivery port 5 (for blowing seeds to different seeding rows), as shown in Figure 1a.

Figure 1b shows the working principle of the device. The power take-off drives the inner (bigger vacuum holes) and outer cylinder to rotate, and the axial fixed ventilation shell has positive and negative pressure cavities. The suction holes of the cylinder in the negative pressure cavity sucks rice seeds in the seed box, and excess rice seeds fall into the seed box under the action of the seeds-cleaning mechanism. The sucked rice seeds enter the positive pressure cavity with the rotation of the cylinder, falling into the seeding tubes under self-weight and positive pressure, and then falling into the sowing furrow [22].

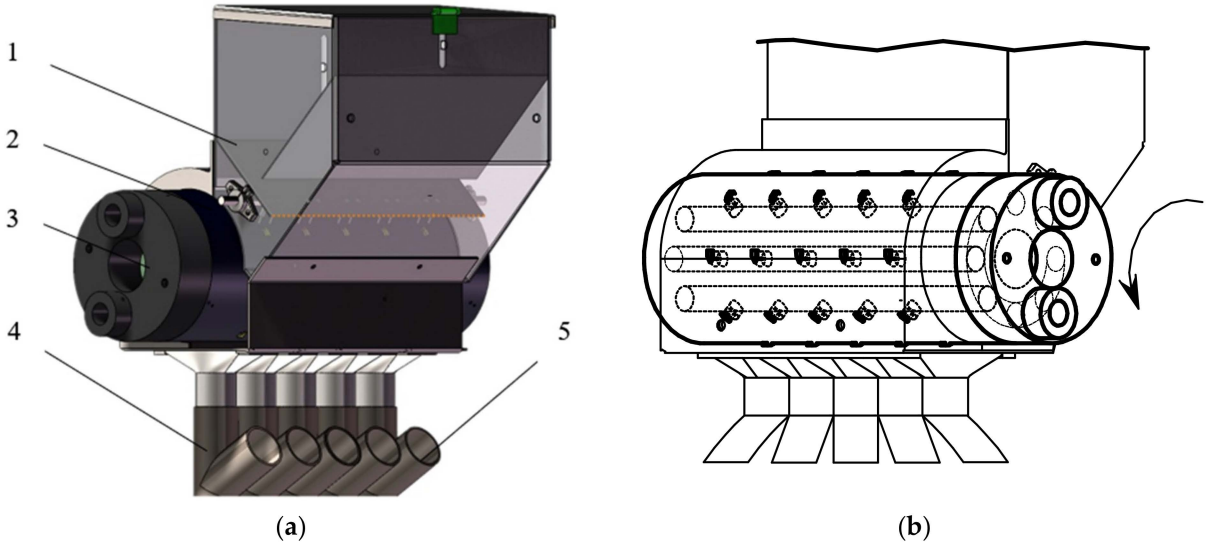

Figure 1. (**a**) Main structure of rice metering device. 1. seed box 2. outer cylinder 3. ventilation shell 4. seeding tubes 5. air delivery ports; (**b**) Schematic diagram of seeding process by vacuum centralized cylinder metering device.

2.2. Design and Simulation of Airflow Distributor Structure

According to the technical requirements of precision seed feeding of a hybrid rice pneumatic centralized cylinder machine, the whole machine adopted the centralized seed row and distributed seed feeding scheme, with one seed-metering device corresponding to five rows of seeding furrows, as shown in Figure 2.

Figure 2. The practicality picture of hill-drop pneumatic central cylinder direct-seeding machine for hybrid rice.

2.3. CFD Simulation of Cylinder Metering Device Cavity

2.3.1. Negative Pressure Seed Suction Area

The physical state parameters of the fluid simulation target are important for the simulation and determination of the air parameters in the cavity and flow channel of the pneumatic seed-metering device. In this study, we assume that the fluid in the pneumatic

metering device is an ideal (non-viscous), Newtonian, incompressible, constant and turbulent flow fluid; the ambient temperature is set at 25°, and the atmospheric pressure is 101,325 Pa.

The stability and uniformity of negative pressure are the key to determine the seed absorption performance of pneumatic seed-metering device. Therefore, this section investigates the uniformity and stability of the negative pressure inside the cavity during the suction process of the seed-metering device to optimize the cavity flow field structure. According to the central cylinder metering device (Figure 3), we extract one of the eight groups of annular suction chambers as the simulation model.

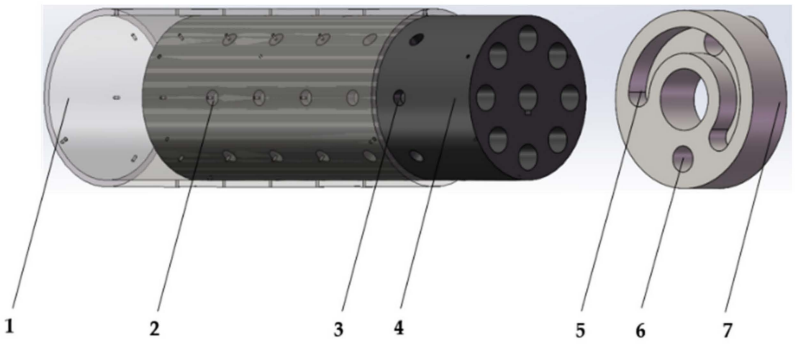

Figure 3. The cylinders and ventilation chamber shell. 1. Outer cylinder; 2. Outer suction holes; 3. Inner cylinder; 4. Inner suction holes; 5. Negative-pressure zone; 6. Positive-pressure zone; 7. Ventilation chamber shell.

The three-dimensional structure model of the suction housing drawn in SolidWorks was saved to x-t format and imported into Ansys-fluent fluid analysis software, which is shown in Figure 4a, and the distribution of the model meshing is shown in Figure 4b. The inlet pressure was 0 Pa and the outlet pressure was −3 kPa; the suction hole sizes of the metering cylinder were set as 2 mm, 1.5 mm and 2.0 mm 45° wedge, respectively, to conduct the fluid dynamics simulation; the flow model was turbulent, the medium was air, and iterative calculations were performed until convergence.

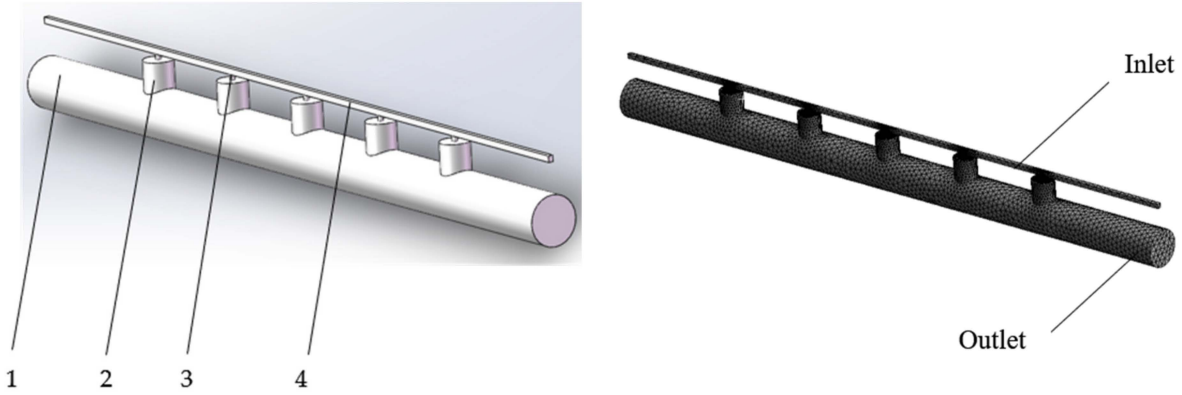

(**a**) (**b**)

Figure 4. (**a**) The physical model and meshing of airflow in negative pressure zone. 1. Airflow field in negative pressure cavity; 2. Airflow field in big suction hole; 3. Airflow field in small suction hole; 4. Airflow field outside the suction hole; (**b**) The meshing of model.

The pressure distribution of a 2 mm hole is shown in Figure 5a; the velocity distribution is shown in Figure 5b; the streamline distribution of the velocity flow field is shown in Figure 5c.

The pressure distribution of a 2 mm 45° wedge hole is shown in Figure 6a; the velocity distribution is shown in Figure 6b; and the streamline distribution of velocity flow field is shown in Figure 6c.

The pressure distribution of the 1.5 mm hole is shown in Figure 7a, the velocity distribution is shown in Figure 7b, and the streamline distribution of velocity flow field is shown in Figure 7c.

As Figures 5–7 show, a CFD airflow field distribution simulation was conducted on the negative pressure area, positive pressure area and airflow distributor of the seed-metering device, and the following conclusions were obtained: the distribution of streamline pressure and velocity in the negative pressure cavity of the seed-metering device is that the internal streamline distribution of the seed-metering device with the 2 mm hole is more uniform than the other two holes, and the pressures at the five holes of the 1.5 mm hole were larger than those of the other two holes, and the pressure values were even under the same negative pressure condition.

The centers of the upper surface of each suction hole were selected and defined as 1, 2, 3, 4 and 5 from left to right. The vacuum values of these points were selected to draw a two-dimensional curve, as shown in Figure 8. Under the same inlet vacuum, the pressure at the 1.5 mm orifice is higher than the other two types of holes, and they vary more steadily than the other two holes. The size of hole affects the distribution of air pressure directly; the smaller the hole, the more negative the pressure increase.

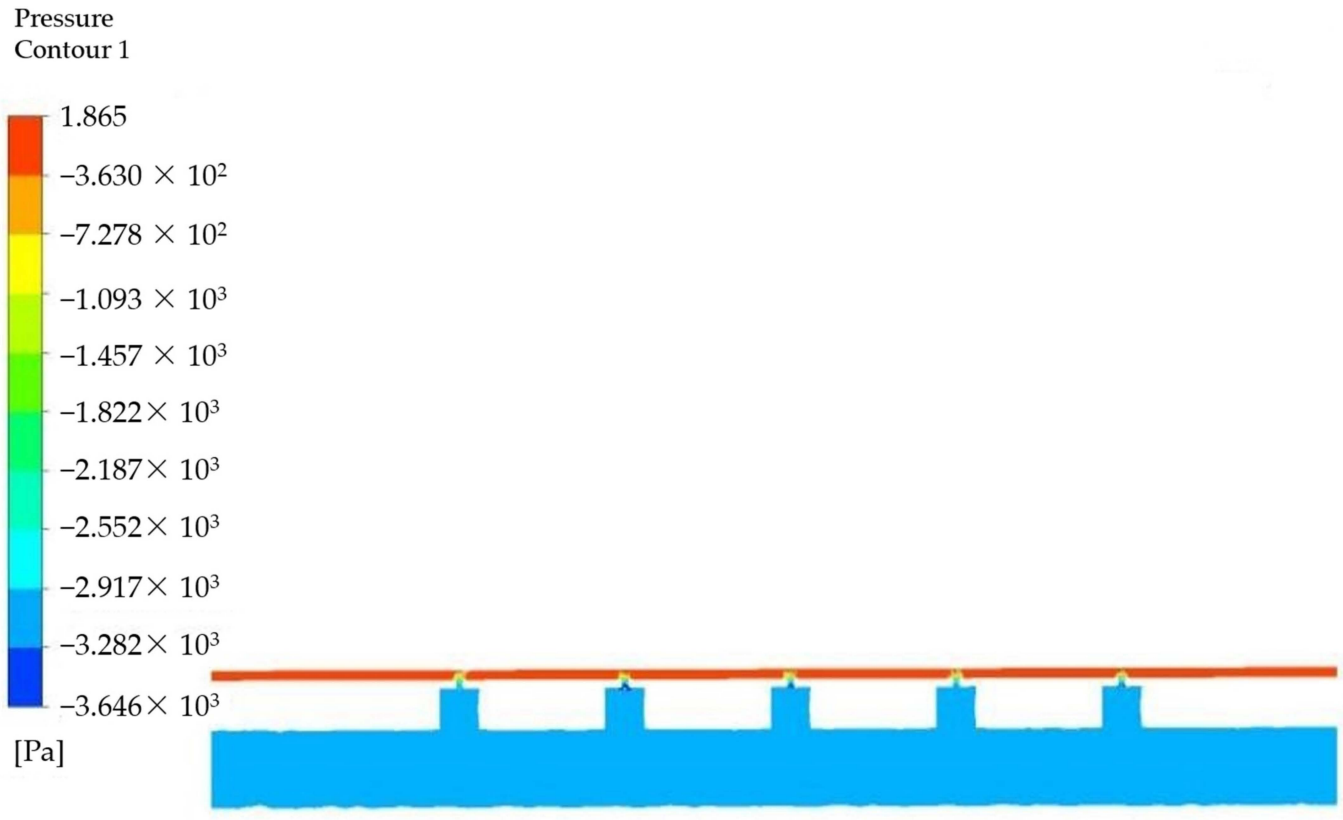

(**a**)

Figure 5. *Cont.*

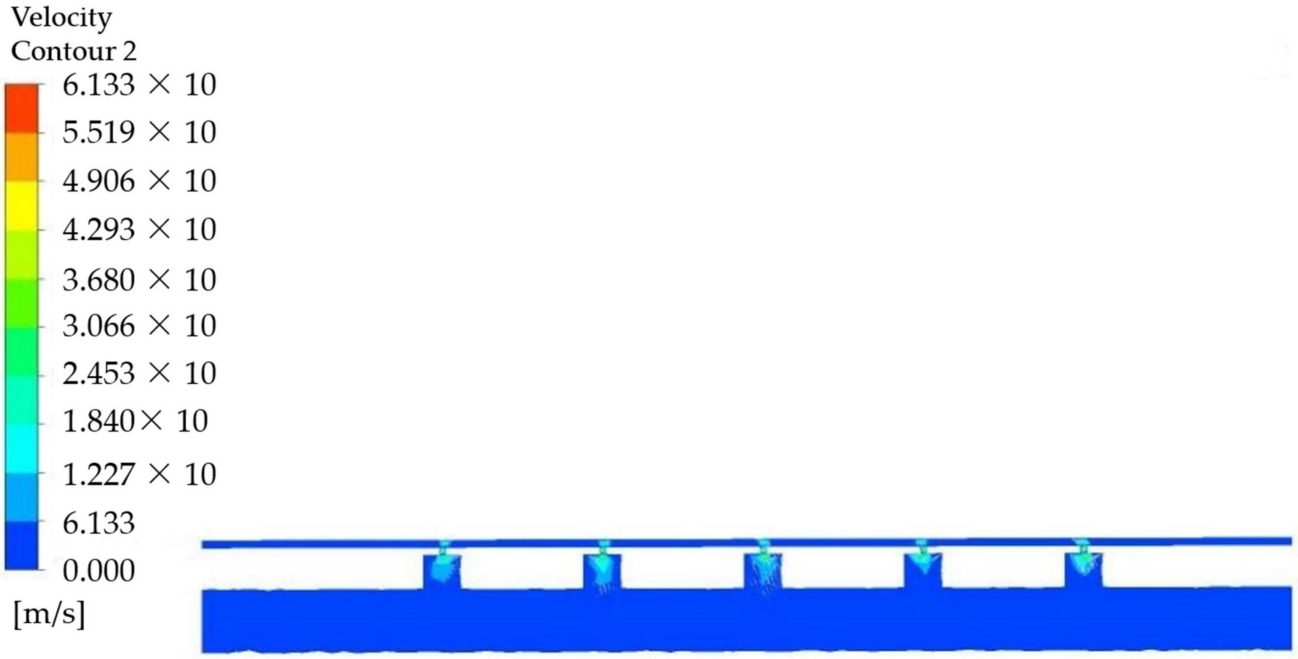

(**b**)

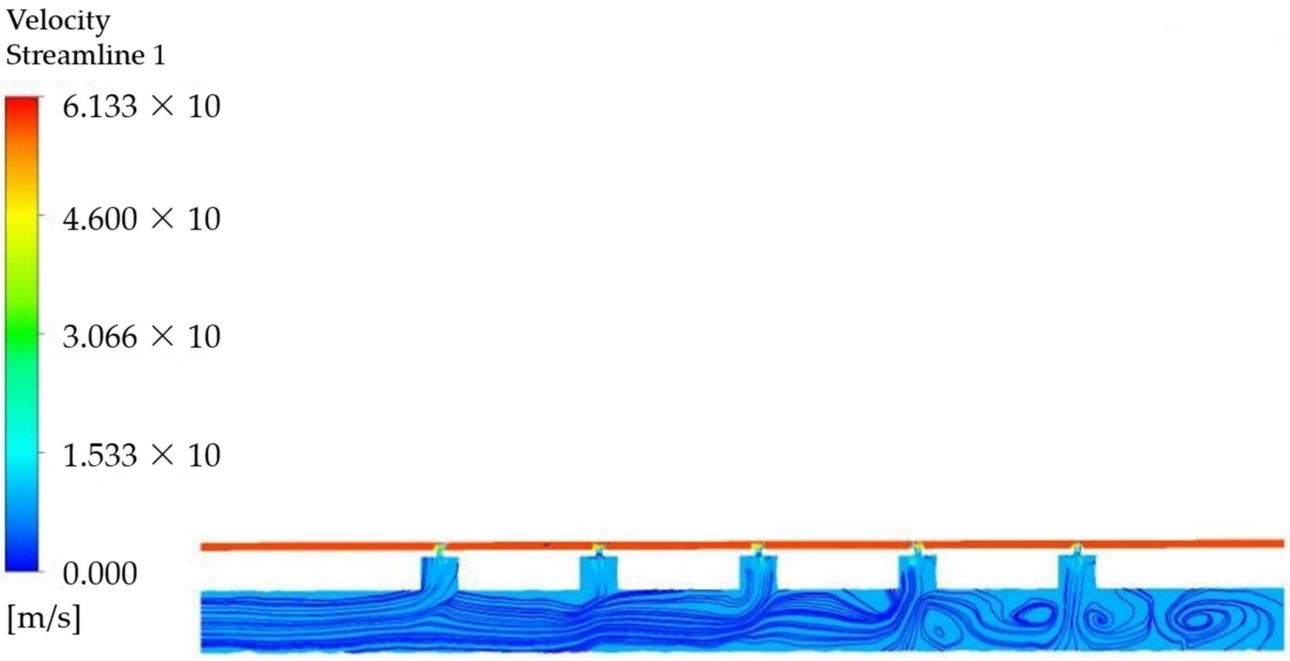

(**c**)

Figure 5. (**a**) The cloud chart of pressure distribution of 2 mm hole; (**b**) The cloud chart of velocity distribution of 2 mm hole; (**c**) The streamline diagram of velocity of 2 mm hole.

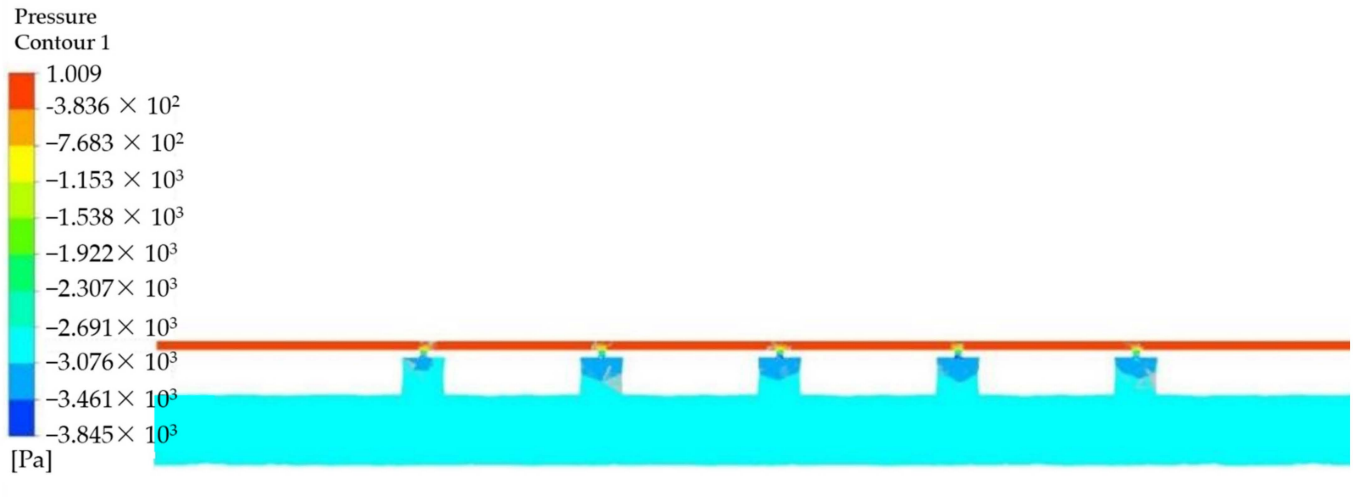

(**a**)

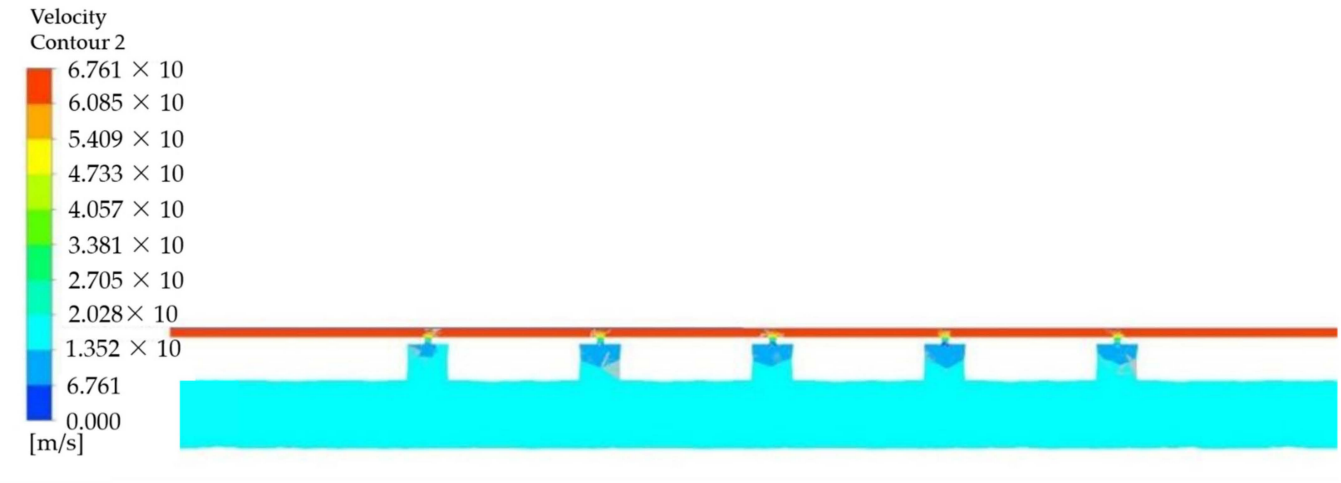

(**b**)

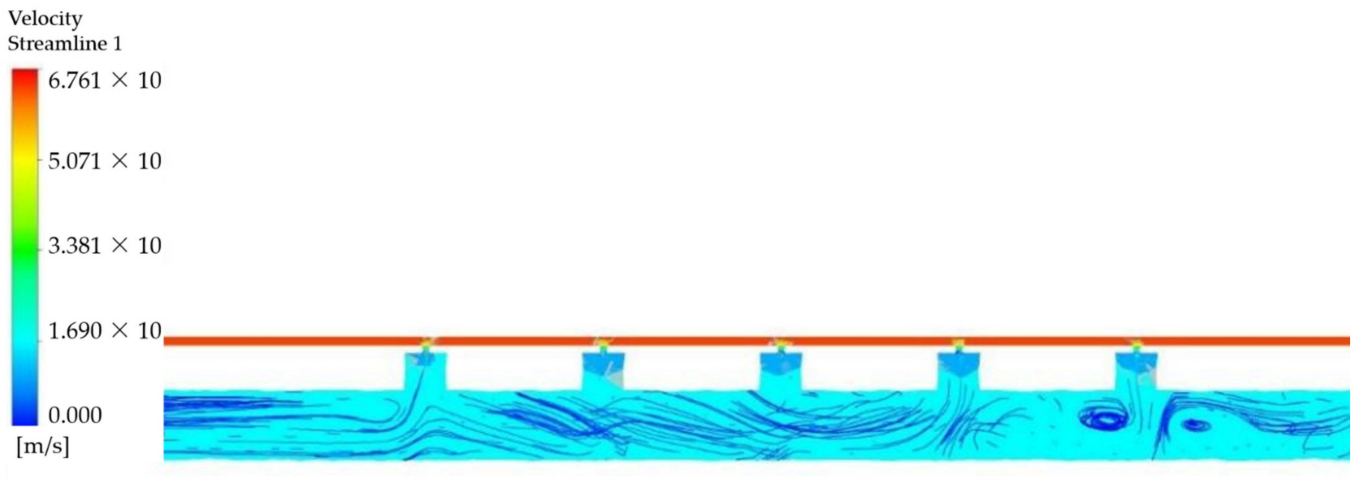

(**c**)

Figure 6. (**a**) The cloud charts of pressure distribution about a 2 mm wedge hole; (**b**) The cloud charts of velocity distribution about a 2 mm wedge hole; (**c**) The streamline diagram of velocity about a 2 mm wedge hole.

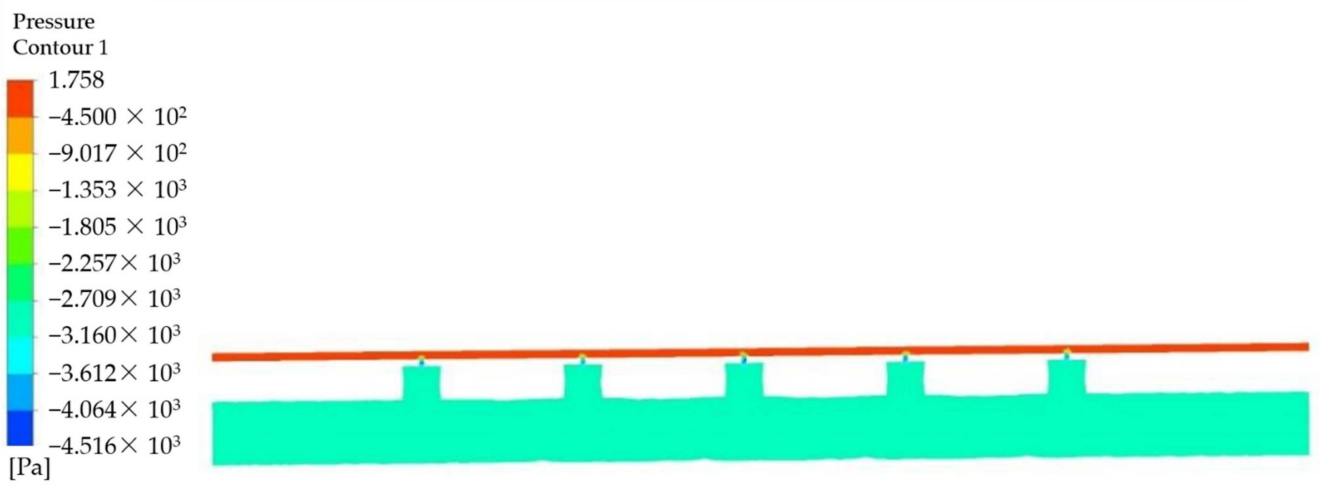

(**a**)

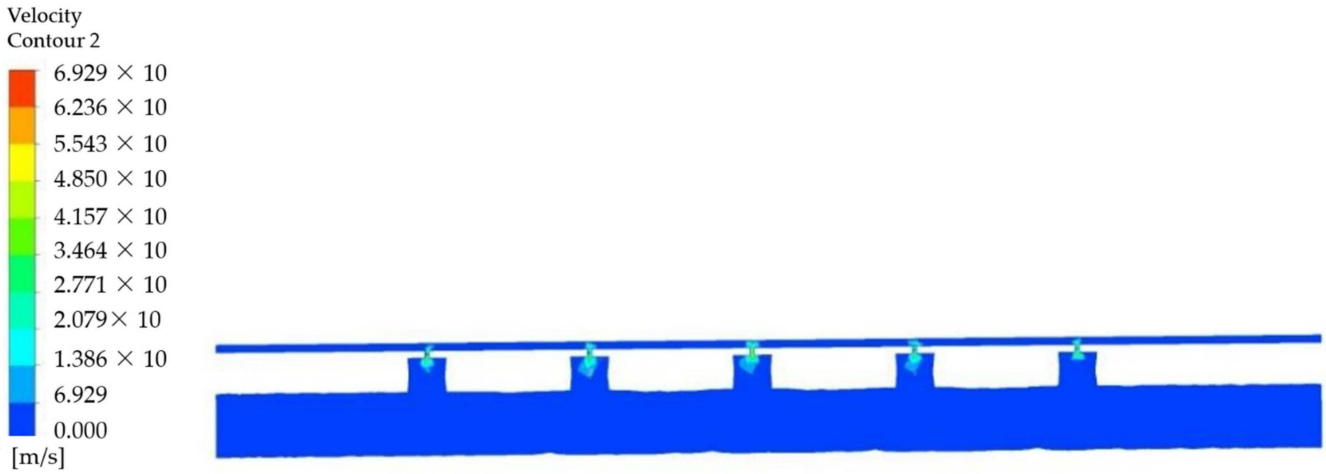

(**b**)

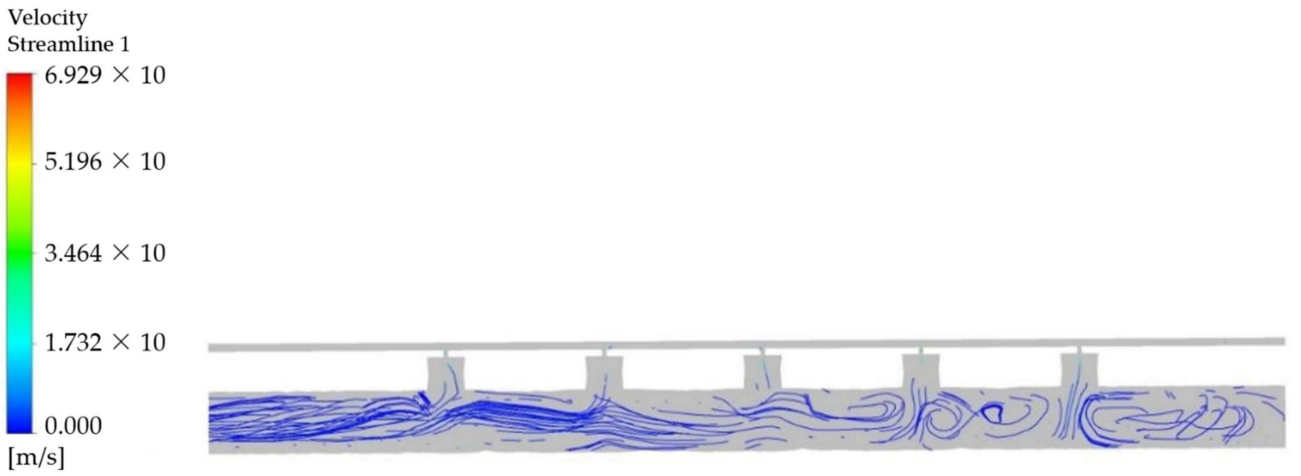

(**c**)

Figure 7. (**a**) The cloud chart of pressure distribution of 1.5 mm; (**b**) The cloud chart of velocity distribution of 1.5 mm hole; (**c**) The streamline diagram of velocity of 1.5 mm hole.

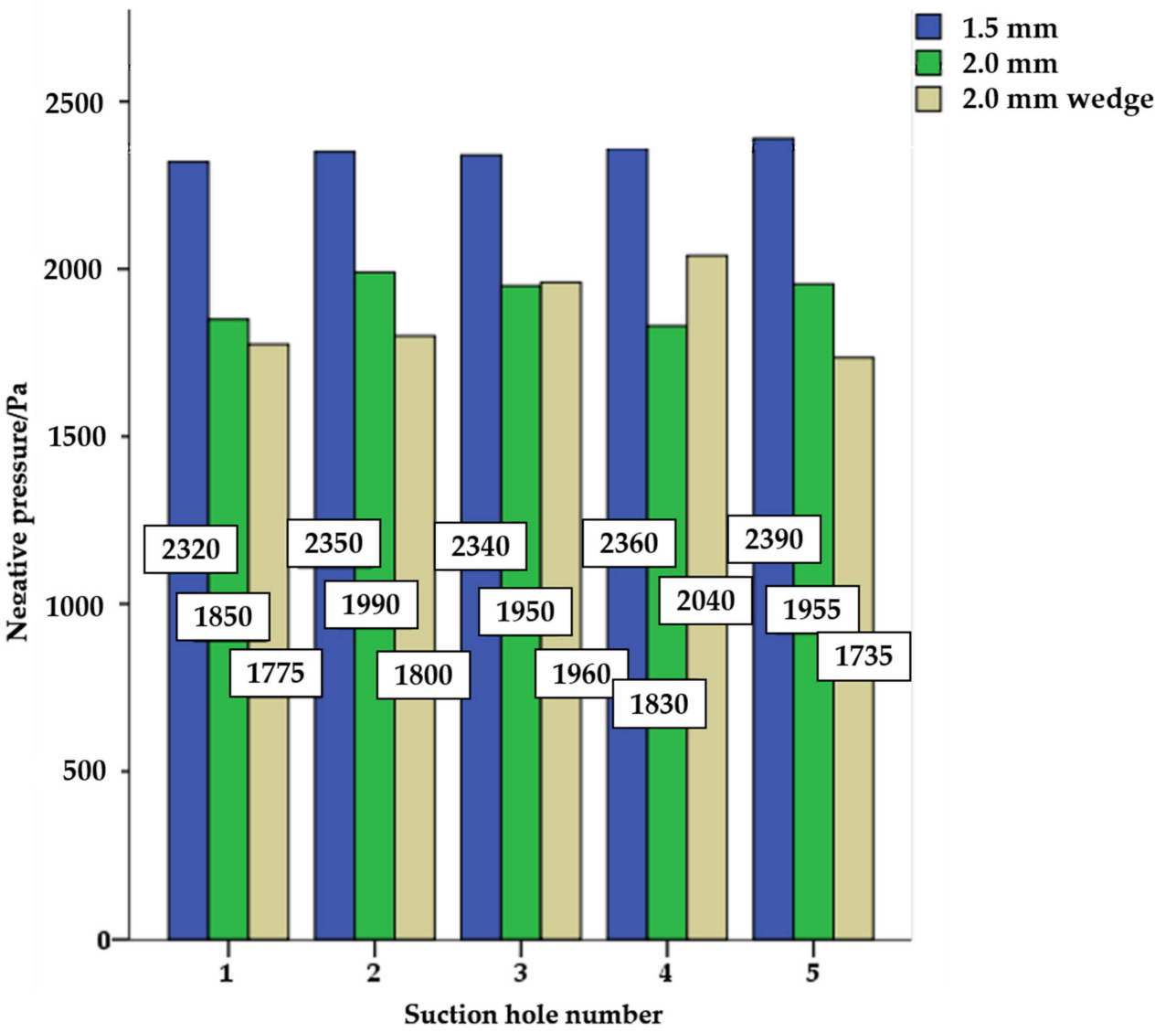

Figure 8. The negative pressure diagram of different hole types with different points.

2.3.2. Positive Pressure Suction Area

When the suction hole carrying seeds rotates to the positive pressure area, the rice seeds fall to the seed feeding tube under the action of gravity and positive pressure, and the uniformity of the flow field distribution in the positive pressure area would directly affect the seed feeding performance. Therefore, this section performs a CFD analysis of the distribution of the flow field in the positive pressure area. The meshing of the three-dimensional structure model is the same as that of the negative pressure area. The inlet and outlet had opposite positions, and the fluent parameter settings were the same as the finite element simulation in the positive pressure area. The inlet pressure was 1.5 kPa and the outlet pressure was 0 Pa.

The pressure distribution of different measurements is shown in Figure 9. As shown, the 2 mm 45° wedge hole had the most uneven distribution, and the overall positive pressure distribution of the 1.5 mm hole was higher than that of the 2 mm hole. Under the same negative pressure condition, the 2 mm hole had more uniform pressure at different suction holes compared with the other two seed feeding cylinders. The above simulation results provided a reference for the optimization of the structural parameters of the positive and negative pressure cavity of seed feeding airflow distributor and seed-metering device.

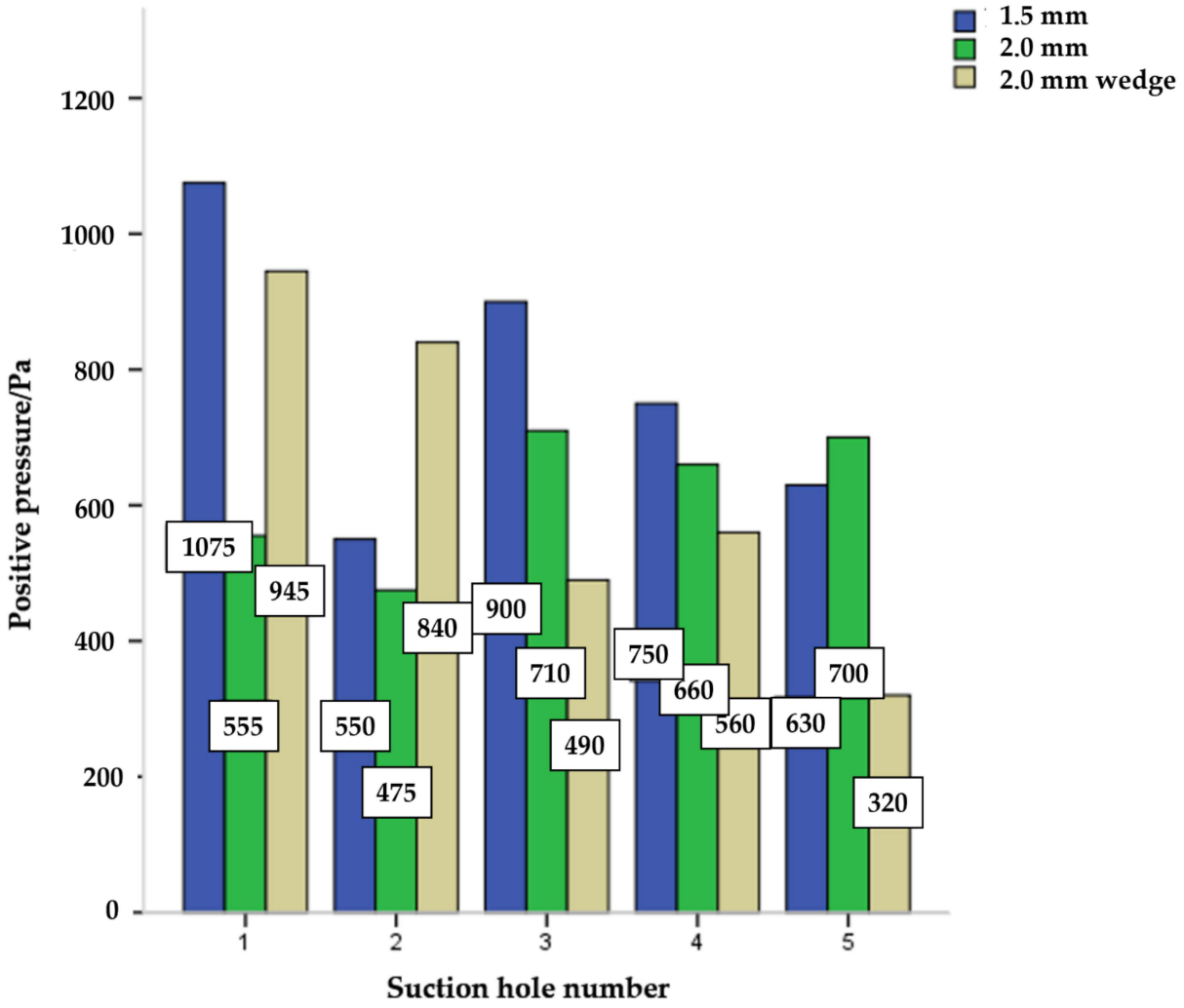

Figure 9. The positive pressure diagram of different hole types with different points.

2.4. Simulation Optimization and Analysis of Pneumatic Positive Pressure Seed Feeding Distributor

According to the sowing characteristics of the pneumatic centralized cylinder rice precision seeding machine, each row of rice would enter the corresponding seed feeding tube after positive pressure seed feeding. The design of the centralized distributed tube required using the pressure feeding pneumatic delivery mode. During the conveying process, the gravity, friction and airflow exerted a certain pressure on the rice seeds, and the airflow is very important to the uniformity of seed feeding. Therefore, simulation optimization and analysis of the airflow uniformity of the positive pressure seed feeding distributor was conducted in this section.

The movement of hybrid rice seeds after discharge from the pneumatic centralized cylinder seed distributor is a gas–solid two-phase flow issue. The ideal state of rice seed movement is that there is no collision between each cavity of rice seeds and uniform movement without stagnation in the tubes, which requires uniform and stable positive pressure conveying pneumatic force, and no small eddy flow was seen. Based on these requirements, three types of positive pressure airflow distributors were designed in this study. The first type is shown in Figure 10A, the five outlets of which were linearly distributed; the second type is shown in Figure 10B, the transition part of which is a cube cavity; the third type is shown in Figure 10C, the transition part of which is a gradual cylindrical shape to avoid pressure and an abrupt velocity change caused by throttling due to the sudden change of cross-sectional area.

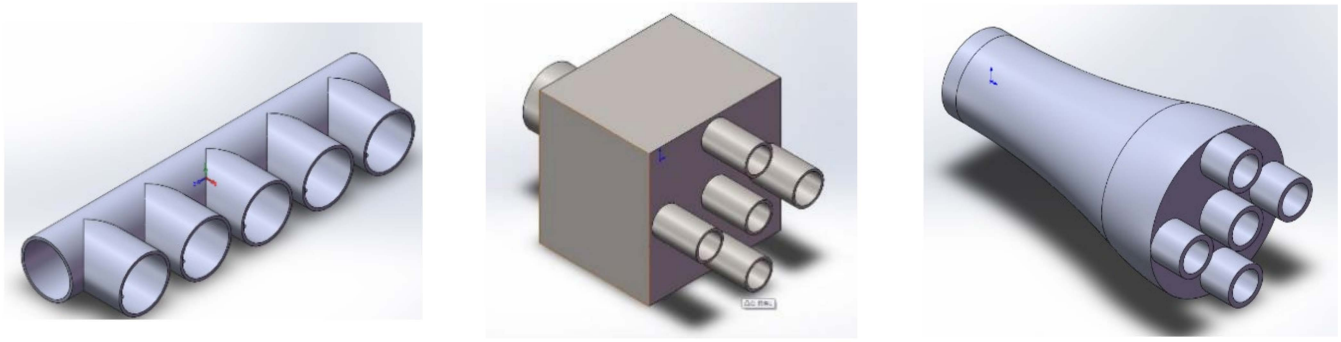

(**A**) (**B**) (**C**)

Figure 10. Different types of airflow distributor. (**A**) Linear type; (**B**) Box type; (**C**) Arc transition type.

First, CFD simulation software Ansys R17.0 was used to study the distribution of the airflow field in the distributor [23–25]. The airflow uniformity and stability between each outlet under different inlet airflow velocities with the same inlet size and inlet flow rate were analyzed. Relevant studies have simulated and experimented the suspending velocity of rice seeds. The suspending velocity of full rice seeds mainly ranged 6–8 m/s [26,27]. According to the multiplicative relationship between the conveying airflow velocity of different conveying structure states and different material settling velocities, the range of positive pressure inlet velocity was set to 8–24 m/s. The experiment factors and level arrangements are shown in Table 1.

Table 1. The schedule of air distributor CFD experiment.

Level	Inlet Velocity (m/s)	Distributor Type
1	8	a
2	16	b
3	24	c

The velocity cloud charts under different airflow velocities and distributors are shown in Figures 11–13. The color distribution of the cloud charts showed that the B-type distributor had the poorest uniformity of airflow; the maximum delivery velocities of the five outlets of the A-type distributor were close, but the outlet velocities were not uniform and eddy flow occurred; the wind velocities between the three outlets of the C-type distributor under three different inlet velocities were uniform, and so were the flow rates of each outlet.

Therefore, this design adopted type (C) arc transition air distributor as the working part, as shown in Figure 14.

2.5. Outlet Airflow Uniformity Experiment at the End of Seed Feeding Tubes

The uniformity and stability of seed delivery between each row of the centralized hybrid rice pneumatic cylinder seed-metering device is very important. Therefore, the airflow uniformity at the end of different seed delivery tubes was conducted in this section based on the transition type seed delivery airflow distributor with different angles of seed feeding tubes and different gasoline-integrated fan throttle openings.

Experiment Items and Methods

The airflow uniformity experiment of 10-row seed feeding tubes was conducted at the Key Laboratory of Key Technology of Southern Agricultural Machinery and Equipment of the Ministry of Education, South China Agricultural University. The distributed seed feeding tube was a 40 mm inner diameter steel wire corrugated tube, as shown in Figure 8. The 2.2 kw power vortex fan throttle opening is divided into 3 gears a, b and c, corresponding to 3 opening degrees of low, medium and high (corresponding to minimum

throttle to maintain operation, medium throttle and max throttle). The three groups of experiments, namely left 5, right 5 and 10 groups were conducted at the same time and repeated 3 times, using an anemometer (Smart sensor AT816; the measurement span is 0.3–30 m/s, the resolution ratio with 0.1, and the measurement error with ±5%) at the outlet. The data were recorded after the airflow velocity indication was stable.

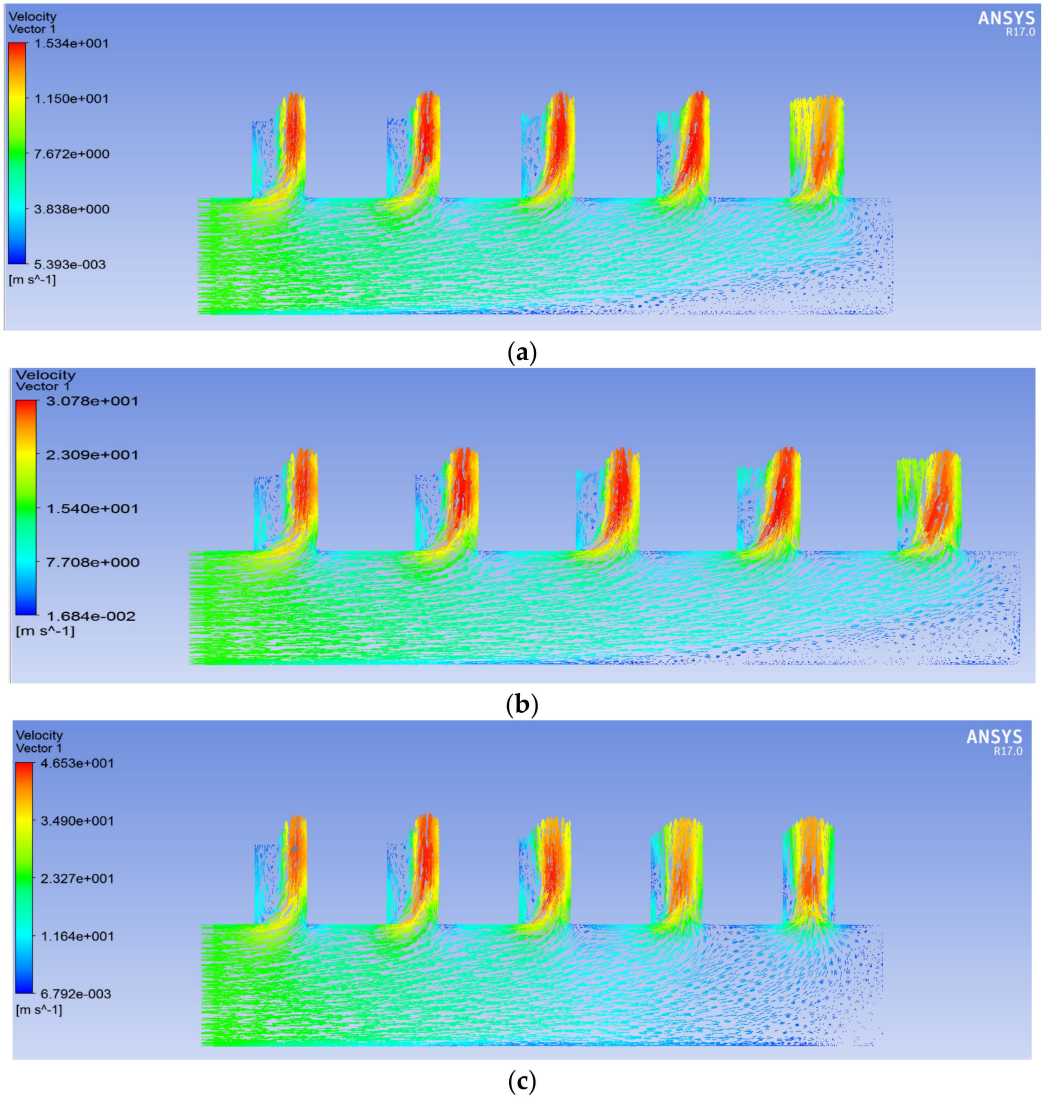

Figure 11. The velocity flow field distribution of different rice distributor CFD simulation with type A. (**a**) 8 m/s inlet velocity; (**b**) 16 m/s inlet velocity; (**c**) 24 m/s inlet velocity.

The airflow velocity uniformity experiments as shown in Tables 2–7 indicated that the airflow velocity was high in the middle and low on both sides, which is consistent with the velocity and flow field simulation results of the airflow distributor.

Table 2. The delivery airflow uniformity experiment of left five tubes. unit: m/s.

	1	2	3	4	5
a	3.155	3.129	4.265	2.609	2.729
b	3.548	3.607	4.673	3.208	3.361
c	6.706	6.721	9.521	5.557	5.770

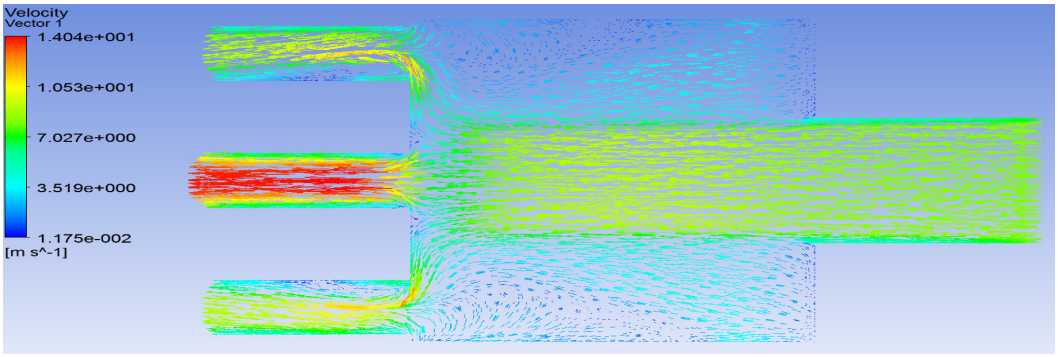

(**a**)

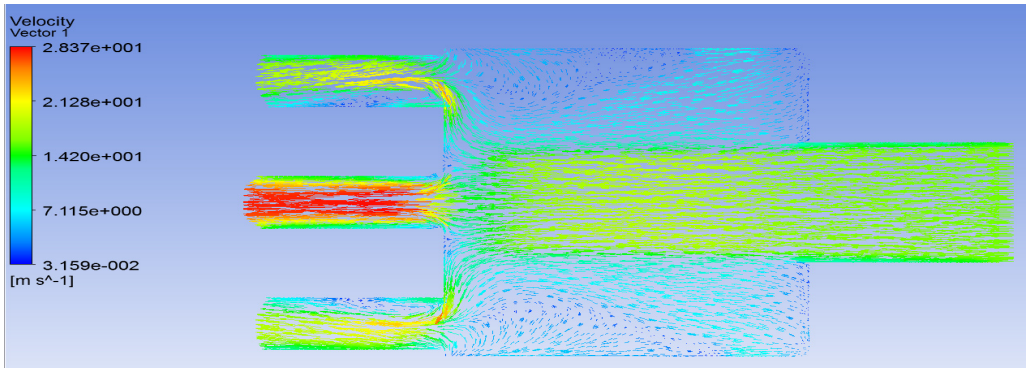

(**b**)

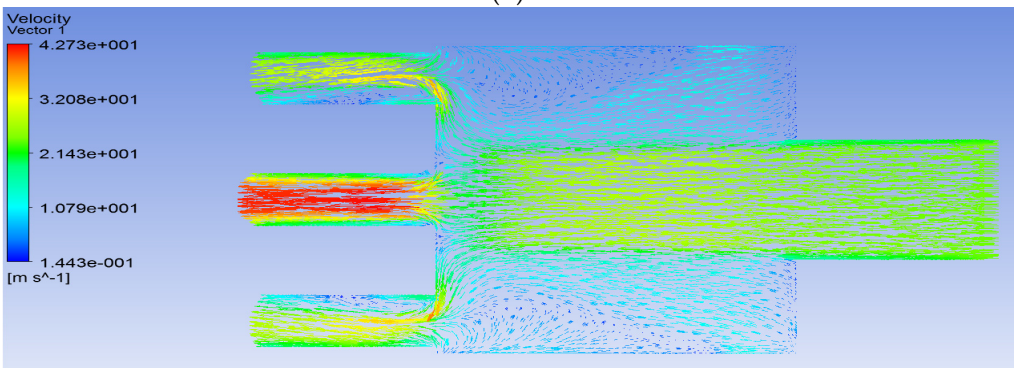

(**c**)

Figure 12. The velocity flow field distribution of different rice distributor CFD simulation with type B. (**a**) 8 m/s inlet velocity; (**b**) 16 m/s inlet velocity; (**c**) 24 m/s inlet velocity.

Table 3. The variability uniformity experiment of left five tubes.

	Standard Deviation	Average Value	Coefficient of Variation
a	0.654	3.177	0.206
b	0.577	3.679	0.157
c	1.582	6.855	0.231

Table 4. The delivery airflow uniformity experiment of right five tubes. unit: m/s.

	6	7	8	9	10
a	2.094	1.903	2.327	1.876	1.874
b	4.044	3.322	4.261	3.355	3.391
c	7.413	6.443	8.080	6.423	5.985

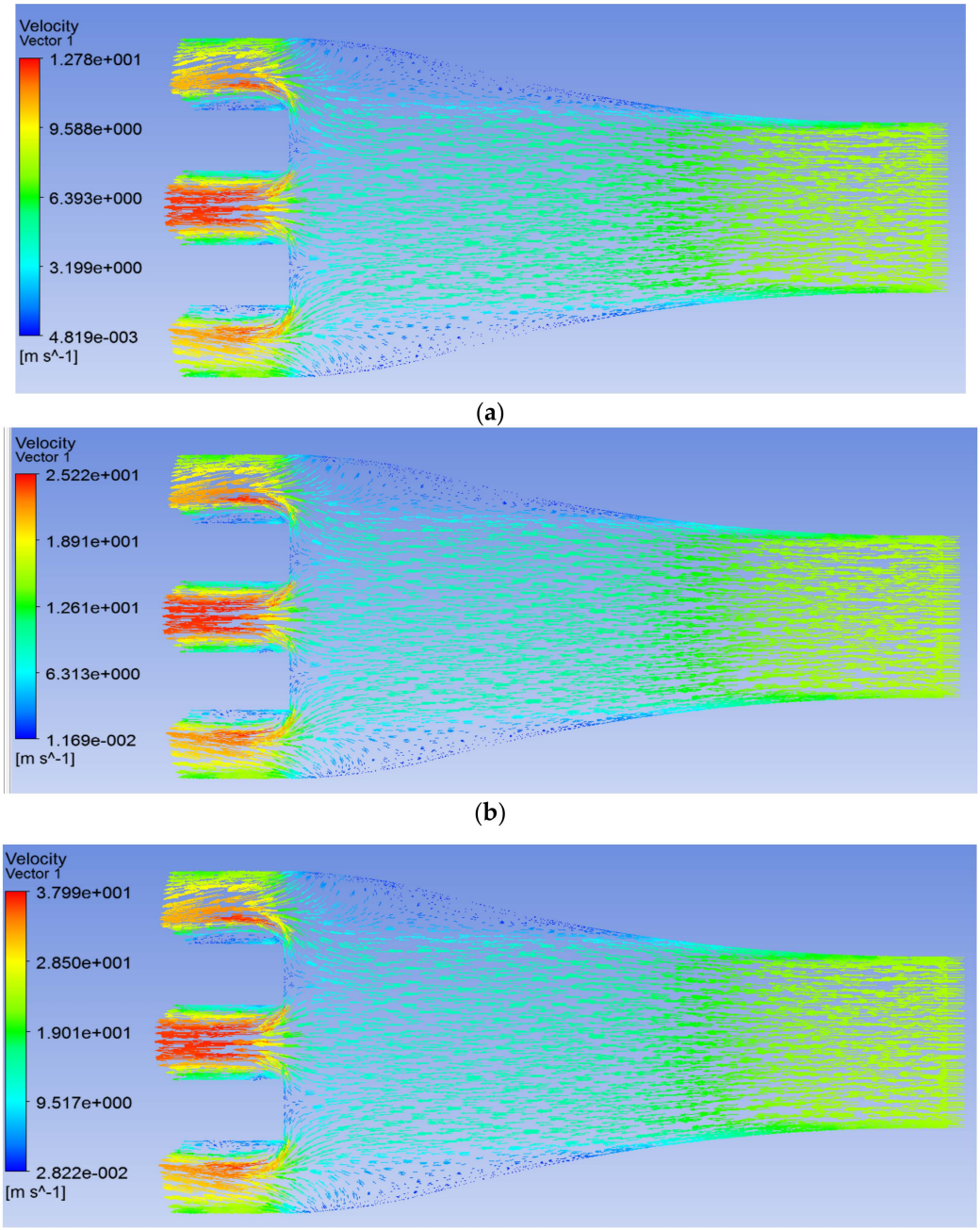

Figure 13. The velocity flow field distribution of different rice distributor CFD simulation with type C. (**a**) 8 m/s inlet velocity; (**b**) 16 m/s inlet velocity; (**c**) 24 m/s inlet velocity.

Table 5. The variability uniformity experiment of right five tubes.

	Standard Deviation	Average Value	Coefficient of Variation
a	0.197	2.015	0.098
b	0.444	3.675	0.121
c	0.855	6.869	0.124

Figure 14. The installation drawing of type (C) arc transition air distributor.

Table 6. The delivery airflow uniformity experiment of ten different delivery tubes. unit: m/s.

	1	2	3	4	5	6	7	8	9	10
a	1.572	1.644	2.212	1.486	1.464	1.826	1.623	1.995	1.639	1.415
b	1.514	1.836	2.364	1.502	1.653	1.952	1.565	2.167	1.562	1.665
c	3.185	3.276	4.469	2.997	2.818	3.625	3.031	4.021	3.018	3.000

Table 7. The variability uniformity experiment of ten different feeding tubes.

	Standard Deviation	Average Value	Coefficient of Variation
a	0.253	1.688	0.150
b	0.297	1.778	0.167
c	0.533	3.344	0.159

When the fan is connected to ten rows at the same time, the airflow velocity had a significant decline, corresponding to low, medium and high throttle openings, and the average airflow velocities at the outlets were only 1.687 m/s, 1.7778 m/s and 3.3441 m/s, respectively, which were far less than the limit airflow velocities of Tables 2 and 4.

2.6. Simulation and Experiment of Distributed Seed-Feeding Tubes

2.6.1. Overall Structure of Distributed Seed-Feeding Tubes

The seed-feeding tubes were symmetrically distributed, with the central tube vertically downward designed, and the seed-feeding tubes (inner size 40 mm) B (maximum angle) and C (the second angle) at different angles were arranged on the left and right sides of the central tube. The cross-point of the central tube and the upper end of the feeding tube was defined as coordinate origin O (0.0); a 2D sketch was drawn with spline curves based on the typical coordinate points obtained from two different angles of distributed tubes, and a 3D tube model was then constructed. The coordinate point data of different seed

feeding tubes are shown in Table 8, and the distribution of the seed feeding tubes is shown in Figure 15.

Table 8. The coordinate point data of different seed-feeding tubes.

Tube C		Tube B	
X (mm)	Y (mm)	X (mm)	Y (mm)
−100	−200	−50	−200
−115	−210	−85	−270
−135	−250	−110	−300
−160	−270	−150	−360
−185	−310	−180	−400
−200	−320	−200	−440
−220	−350	−250	−565
−250	−370		
−270	−380		
−300	−390		
−350	−400		
−400	−440		
−450	−450		
−500	−565		

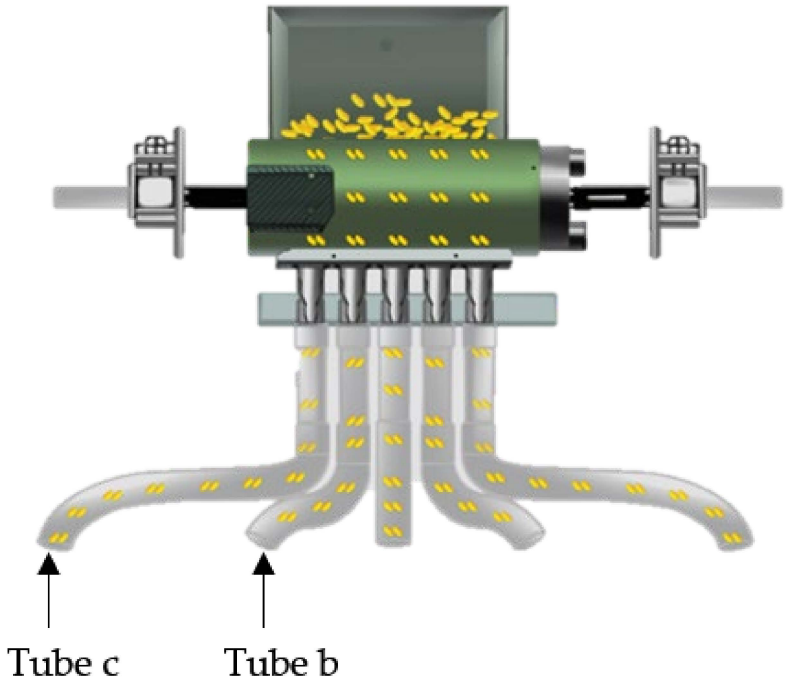

Figure 15. The schematic diagram of distributed seed-feeding tubes.

2.6.2. Study on the Movement Law of Rice Seeds

The movement law and seed-metering mechanism were obtained by using high-speed photography to record the process of the rice seeds entering the seed feeding tubes, colliding with the tube wall and exiting the tubes [28,29]. The movement posture and other indicators of the rice seeds were analyzed based on the high-speed photography experiment of the movement time and posture of rice seeds.

During the photography experiment (speed: 250 fps; resolution: 1024 × 1024), the delivery state and falling process of the 1000 rice seeds in tube C and tube B at different inlet velocities were observed and recorded, and a statistic analysis was performed. The experiment devices are shown in Figure 16.

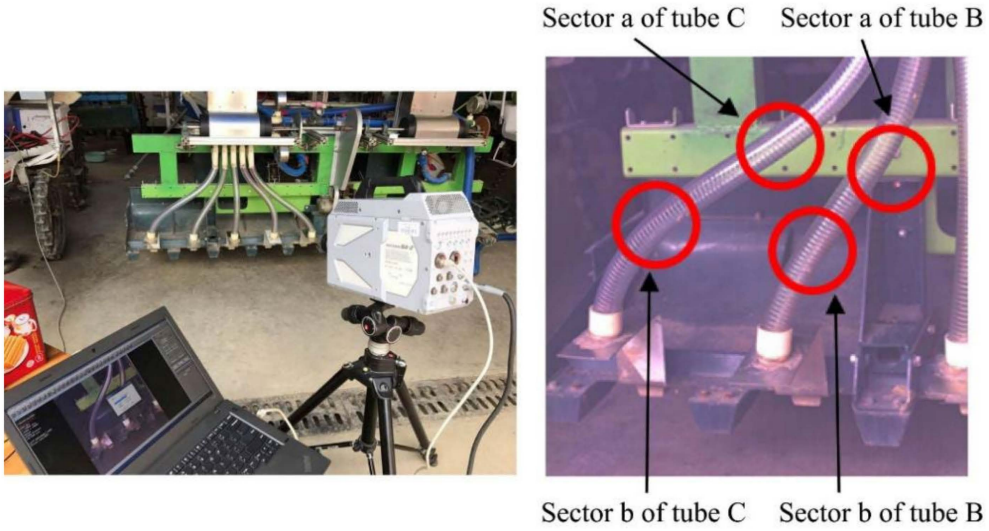

Figure 16. The high-speed photography of rice seed movement state with different tube angles. (**a**) Seed delivery experiment; (**b**) The division of collision zone.

The analysis and calculation were carried out according to the pneumatic conveying theory. The seed feeding velocity of 8–40 m/s was selected as the variation range of experiment factor of airflow feeding velocity. The schedule of the experiment is shown in Table 9.

Table 9. The schedule of air CFD experiment for seed feeding.

Level	Inlet Velocity (m/s)	Type of Seed Feeding Tubes
1	8	C
2	16	B
3	24	
4	32	
5	40	

First, the collision zone was divided based on the angle change of tube C and tube B, as shown in Figure 16b. The movement of rice seed in the delivery tube was the last stage of the whole seed delivery process as well as the last influence part of field distribution state. According to the analysis of the seed delivery state based on high-speed photography, the movement posture of the rice seeds during the falling process mainly included the following types:

① Falling in both Sector a and Sector b;
② Falling in Sector a, colliding with Sector b and then falling;
③ Colliding with Sector a and falling directly without collision with Sector b;
④ Colliding with both Sector a and Sector b and then falling.

The movement trajectory of 1000 rice seeds (rice varieties Jingliangyou1212) at different airflow velocities in the seed feeding tubes was analyzed using the high-speed photography method. The collision probability results are shown in Table 10.

Table 10. The schedule of movement posture probability for seed delivery. unit: (%). (**a**) airflow velocity: 8 (m/s); (**b**) airflow velocity: 16 (m/s); (**c**) airflow velocity: 24 (m/s); (**d**) airflow velocity: 32 (m/s); (**e**) airflow velocity: 40 (m/s).

Tube Type	a				b				c			
	①	②	③	④	①	②	③	④	①	②	③	④
Tube C	30.4	56.5	4.3	8.8	0	87.0	3.0	10	0	64.9	0	25.1
Tube B	38.5	61.5	0	0	33.3	35.7	4.8	26.2	10.5	55.3	2.6	31.6
Tube Type	d				e							
	①	②	③	④	①	②	③	④				
Tube C	0	56.5	4.3	39.2	0	47.7	0	52.3				
Tube B	0	53.5	23.3	23.2	0	41.2	0	58.8				

3. Discussion

In order to promote the level of lightened and simplified mechanization of hybrid rice direct seeding, this paper adopted a combination of CFD simulation, mechanism design and experimental analysis to study the pressure and flow field distribution as well as the movement law of rice seeds in the delivery tubes.

3.1 The pressure distribution inside the cavity had a direct effect on the performance of the seed-metering device. In this paper, the CFD simulation method was used to analyze the uniformity of pressure distribution at different diameter suction holes of the tubes of the same metering device to obtain the hole parameters with optimal air pressure uniformity. In the next step, more parameters can be taken into account, such as the shape of the hole, etc.

3.2 The uniformity of airflow velocity in the distributed seed delivery tubes had a direct impact on the movement of rice seeds, so the structure of the airflow distributor is particularly important. This paper designed three typical airflow distributors as its basis and performed the simulation and experimental analysis with different inlet airflow velocities as the influencing factors, aiming to select the airflow distributor with more uniform airflow distribution. Having analyzed different types of airflow distributors, the selected airflow distributor parameters need further study.

3.3 The movement of rice seeds in the seed delivery tube was the last and also most critical process of sowing. In this paper, the movement of rice seeds in the tube with different angles of the seed-feeding tube and different airflow speed of seed delivery was analyzed to determine the collision law of the rice seeds. The form of distribution of the seed delivery tubes, their angle and the avoidance of sliding friction coefficients with the seeds all affected the distribution of the seeds in the field, which is the focus of future research. For future experiments, the fitting equation can be established to analyze the relationship between the angle and the motion probability of seeds.

4. Conclusions

4.1 The fluid dynamics simulation was performed with the settings of inlet pressure of 0 Pa, outlet pressure of −3 kPa, hole sizes of the seed delivery cylinder of 2 mm, 1.5 mm and 2.0 mm wedge. Under the same inlet vacuum, the pressure at the 1.5 mm hole is higher than the other two types of holes, and the five measurement points of the 2 mm hole were more stable than the other two holes. The results showed that the air pressure and airflow distribution of the 2 mm diameter hole were more uniform than the other two.

4.2 The uniformity of the three types of seed delivery airflow distributors was compared by CFD simulation analysis with 8,16,24 m/s inlet airflow velocity as the experiment factors, and the airflow uniformity of the 10-row seed delivery tubes was experimented. The gasoline engine throttle openings were divided into three grades, and the velocity at tube end was recorded by an anemometer. The results showed that the arc transition type seeding delivery distributor can provide uniform airflow pressure and velocity for seed delivery tubes with different angles.

4.3 The rice seeds in tube C (maximum angle) presented a movement posture of falling sector a and keeping falling after colliding in sector b; the rice seeds in tube B (the second angle) presented a movement posture of falling in sector a and keeping falling after colliding in sector b.

5. Patents

Three patents have been applied in China in this manuscript (Patent No. CN201610027389.8/No. CN201721420260.X and No. CN201620577827.3).

Author Contributions: Conceptualization, X.L.; methodology, B.W.; software, B.W.; validation, Y.N.; formal analysis, B.W.; investigation, Y.P.; resources, X.L.; data curation, Y.N.; writing—original draft preparation, Y.N.; writing—review and editing, B.W.; visualization, Z.G.; supervision, J.L.; project administration, X.L.; funding acquisition, B.W. All authors have read and agreed to the published version of the manuscript.

Funding: This research was funded by Hainan Provincial Natural Science Foundation of China, grant number 520RC551; Hainan University Scientific Research Fund, grant number KYQD(ZR)20054.

Institutional Review Board Statement: Not applicable.

Informed Consent Statement: Not applicable.

Data Availability Statement: All data are presented in this article in the form of figures and tables.

Conflicts of Interest: The authors declare no conflict of interest.

Nomenclature

CFD	Computational Fluid Dynamics

References

1. Luo, X.; Jiang, E.; Wang, Z.; Tang, X.; Li, J.; Chen, W. Precision rice hill-drop drilling machine. *Trans. Chin. Soc. Agric. Eng.* **2008**, *24*, 52–56.
2. Zeng, S.; Tang, H.; Luo, X.; Ma, G.; Wang, Z.; Zang, Y.; Zhang, M. Design and experiment of precision rice hill-drop drilling machine for dry land with synchronous fertilizing. *Trans. Chin. Soc. Agric. Eng.* **2012**, *28*, 12–19.
3. Singh, R.; Gite, L. Technological Change in Paddy Production: A Comparative Analysis of Traditional and Direct Seeding Methods of Cultivation. *AMA-Agric. Mech. Asia Afr. Lat. Am.* **2012**, *43*, 41–46.
4. Dixit, A.; Manes, G.; Singh, A. Evaluation of direct-seeded rice drill against Japanese manual transplanter for higher productivity in rice. *Indian J. Agric. Sci.* **2010**, *80*, 884–887.
5. National Bureau of Statistics of the People's Republic of China. Annual Data, Rice Sown Area (Thousand Hectareas). Available online: https://data.stats.gov.cn/easyquery.htm?cn=C01 (accessed on 20 May 2022).
6. Hu, Z.; Tian, Y.; Xu, Q. Review of Extension and Analysis on Current Status of Hybrid Rice in China. *Hybrid Rice* **2016**, *312*, 1–8.
7. Zhang, G.; Zang, Y.; Luo, X.; Wang, Z.; Li, Z. Line-churning tooth design and metering accuracy experiment of rice pneumatic precision hill- drop seed-metering device on pregnant Japonica rice seed. *Trans. Chin. Soc. Agric. Eng.* **2014**, *30*, 1–9.
8. Zhang, G.; Zang, Y.; Luo, X.; Wang, Z.; Zeng, S.; Zhou, Z. Design and experiment of oriented seed churning device on pneumatic seed-metering device for rice. *Trans. Chin. Soc. Agric. Eng.* **2013**, *29*, 1–8.
9. Zhang, G.; Luo, X.; Zang, Y.; Wang, Z.; Zeng, S.; Zhou, Z. Experiment of sucking precision of sucking plate with group holes on rice pneumatic metering device. *Trans. Chin. Soc. Agric. Eng.* **2013**, *29*, 13–20.
10. Xing, H.; Zang, Y.; Wang, Z.; Luo, X.; Zhang, G.; Cao, X.; Gu, X. Design and experiment of stratified seed- filling room on rice pneumatic metering device. *Trans. Chin. Soc. Agric. Eng.* **2015**, *31*, 42–48.
11. Lei, X.; Liao, Y.; Li, Z.; Zhang, W.; Li, S.; Liao, Q. Design of seed churning device in air-assisted centralized metering device for rapeseed and wheat and experiment on seed filling performance. *Trans. Chin. Soc. Agric. Eng.* **2016**, *32*, 26–34.
12. Liu, Y.; Zhao, M.; Liu, F.; Yang, T.; Zhang, T.; Li, F. Simulation and Optimization of Working Parameters of Air Suction Metering Device Based on Discrete Element. *Trans. Chin. Soc. Agric. Mach.* **2016**, *47*, 65–72.
13. Xiong, D.; Wu, M.; Xie, W.; Liu, R.; Luo, H. Design and Experimental Study of the General Mechanical Pneumatic Combined seed-metering Device. *Appl. Sci.* **2021**, *11*, 7223. [CrossRef]
14. Guo, H.; Cao, Y.; Song, W.; Zhang, J.; Wang, C.; Wang, C.; Yang, F.; Zhu, L. Design and Simulation of a Garlic seed-metering Mechanism. *Agriculture* **2021**, *11*, 1239. [CrossRef]
15. Zhao, Z.; Li, Y.; Chen, J.; Zhou, H. Dynamic analysis on seeds pick-up process for vacuum-cylinder seeder. *Trans. Chin. Soc. Agric. Eng.* **2011**, *27*, 112–116.

16. Zuo, Y.; Ma, X.; Qi, L.; Yu, D.; Liao, X. Seeding experiments of suction cylinder-seeder with socket-slot. *Trans. Chin. Soc. Agric. Eng.* **2010**, *26*, 141–144.
17. Zuo, Y.; Ma, X.; Yu, D.; Liao, X. Flow Field Numerical Simulation of Suction Cylinder-seeder for Rice Bud Seed with Socket slot. *Trans. Chin. Soc. Agric. Mach.* **2011**, *42*, 58–62.
18. Gao, X.; Zhou, J.; Lai, Q. Design and experiment of pneumatic cylinder precision seed- metering device for panax notoginsen. *Trans. Chin. Soc. Agric. Eng.* **2016**, *32*, 20–28.
19. Hu, J.; Zheng, S.; Liu, W. Design and Experiment of Precision Magnetic Cylinder-seeder. *Trans. Chin. Soc. Agric. Eng.* **2009**, *3*, 60–63.
20. Wang, B.; Na, Y.; Liu, J.; Wang, Z.; Zheng, L.; Zhang, M.; Dai, Y.; Xing, H. Design and Evaluation of Vacuum Central Drum Seed Metering Device. *Appl. Sci.* **2022**, *12*, 2159. [CrossRef]
21. Wang, B.; Luo, X.; Wang, Z. Design and field evaluation of hill-drop pneumatic central cylinder direct-seeding machine for hybrid rice. *Int. J. Agric. Biol. Eng.* **2018**, *11*, 33–40. [CrossRef]
22. Wang, B.; Wang, Z.; Luo, X.; Zhang, M.; Fang, L.; Liu, S.; Xu, P. Design and experiment of wedge churning device for pneumatic cylinder-type seed metering device for hybrid rice. *Trans. Chin. Soc. Agric. Eng.* **2019**, *35*, 1–8.
23. Dai, Y.; Luo, X.; Wang, Z.; Zeng, S.; Zang, Y.; Yang, W.; Zhang, M.; Wang, B.; Xing, H. Design and experiment of rice pneumatic centralized seed distributor. *Trans. Chin. Soc. Agric. Eng.* **2016**, *32*, 36–42.
24. Choi, C.; Lee, C.; Kim, I.S. Modeling of flow uniformity by installing inlet distributor within the inflow part of a pressurized module using computational fluid dynamics. *Environ. Eng. Res.* **2020**, *25*, 969–976. [CrossRef]
25. Afshari, F.; Sözen, A.; Khanlari, A.; Tuncer, A.D.; Şirin, C. Effect of turbulator modifications on the thermal performance of cost–effective alternative solar air heater. *Renew. Energy* **2020**, *158*, 297–310. [CrossRef]
26. Liu, Y.; Li, Y.; Xu, L.; Li, H. Experimental Study on Rice Floating Velocity. *J. Agric. Mech. Res.* **2010**, *32*, 149–151 + 155.
27. Su, W.; Gao, X.; Ren, C.; Lai, Q. A simulation prediction method of suspension speed of seed particle swarm. *J. South China Agric. Univ.* **2016**, *37*, 110–116.
28. Pan, B.; Qian, K.; Xie, H.; Asundi, A. Two–dimensional digital image correlation for in–plane displacement and strain measurement: A review. *Meas. Sci. Technol.* **2009**, *20*, 062001. [CrossRef]
29. Shao, C.; Gu, B.; Zhou, J.; Cheng, W. Internal flow measurement in centrifugal pump by high-speed photography and error analysis. *Trans. Chin. Soc. Agric. Eng.* **2015**, *31*, 52–58.